

Effect of charge load proportion and blast controllable factor design on blast fragment size distribution

Blessing Olamide Taiwo*

Department of Mining Engineering, Federal University of Technology Akure, Nigeria

Keywords

Charge load ratio,
Maximum instantaneous charge,
De-normalization,
Blast fragmentation,
Wipfrag software.

Abstract

Blasting operation involves the use of a specific explosive quantity, detonated to fragment insitu and oversize rock block for particle reduction. Rock fragmentation size distribution has a direct influence on the proposed costs of mining one ton of the ore and the cost of run-off-mine processing. The focus of this study is on investigating the effect of charge load ratio and blast design parameters such as stiffness ratio, maximum instantaneous charge, and specific charge on rock fragmentation particle size distribution in dolomite quarry located at Akoko Edo state, South-west Nigeria. The 50% passing sizes (X_{50} , m), 80% passing size (X_{80} , m), and characteristic size (X_c , m) of blast results were determined using Wipware software. It was observed that the optimum mean size (X_{50} , m), 80% passing fragment size (X_{80} , m), and characteristic size (X_c , m) of rock depends strongly on the explosive bottom and column loading ratio, stiffness ratio, and specific charge. The regression analysis result reveals that the explosive specific charge and stiffness ratio influence the fragment size distribution with a negative correlation relationship, and the explosive bottom and column loading ratio has a positive correlation relationship with the blast fragmentation. Multivariate Regression (MVR) models were developed for the prediction of blast fragmentation sizes (X_{80} , X_{50} , and X_c) with R^2 values of 0.76, 0.52, and 0.63 respectively. Based on the low correlation value obtained from the developed models, the proposed multivariate Regression (MVR) models are less suitable for the prediction of blast fragmentation particle size distribution.

1. Introduction

Industrial rock mass and rock bearing ore exist as huge materials within the earth's crust, it is found at shallow or deep depth depending on the mineral mode of formation and the kind of post-formational effects it is exposed to with time. According to Brady and Brown, [1], rock formation differs from all different engineering materials as a result it contains fractures that render its structural existence discontinuous. Although there's forever a desire for a correct blasting design for the exploitation of ore deposits, several controllable factors must be considered to control the rock heterogeneousness characteristics. The perfection of a blasting operation is set by the degree of matching the blast result and also the needed fragment size with the first processing crusher gape size. Blast fragmentation potency and demand specifications square measure sometimes ruled by loading equipment, transport equipment, and significantly the primary crushing units.

[2-3] work established that the efficiency of all the sequential mining operations after blasting depends firmly on blast result size distribution. According to [4] and [5], drilling and blasting operation square measure the extent of getting an optimum blast size distribution, and way of economizing total mining operation cost. In mine wherever blasting operation isn't properly monitored and controlled, it will enhance the assembly value and have an effect on the production process because of unneeded secondary blasting, selective loading, reduction in loader utilization issues and increase in downstream operation value. [6] indicated that to minimize the cost of mining and reduce the operating time blasting design has to take proper consideration at the preplanning stage so as to simulate the rock fragment. According to [7], the operation cost incurred on drilling and blasting in an open-pit mine account for over 15-20% of the mining value. In most exhausting rock mining strategies, drilling and blasting are the most generally used technique for

fragmenting the rock mass for handling (transportation and storage for processing). A good blasting result is described by [8] as that which yields the downstream specific fragmentation in an exceedingly safe, economic, and environmentally friendly manner. In order ways, a poorly conducted blast turn into poor fragmentation and adverse effects such as high percentage oversize, fly rocks generation, ground vibration, airblast, and back break. [8] additionally established that blasting operation is capital intensive and capital overwhelming preferable to other mine operations due to; the necessity for rock mass reduction at hand ready sizes; economical use of explosive energy at a high safety level; and management of blasting to avoid oversized materials. The first prerequisite for any blast design square measure is to confirm optimum results for existing operative conditions, possess adequate flexibility, and are relatively straightforward to use [10]. The two widely identified factors affecting blast design result efficiency are;

- i. Uncontrollable factors; and,
- ii. Manageable or Controllable factors.

The determination of blasting result efficiency is necessary to control explosive charge energy utilization and to avoid any form of energy loss to environmental damage [11]. Analyzing Fragmentation has been proven useful in the mining, construction, and aggregate industries as a means to help to minimize mining costs, improve loader's diggerability, and haulage efficiency, and minimize time down due to selective loading [10]. [11] indicated that Mine-to-Mill operation assesment process is one of the approaches use in optimizing blasting operation in order to accomplish energy and cost minimization. This approach involves sampling and modeling of blasting and processing, followed by the simulation to optimize the operation and develop alternatives [11]. There are several fragmentation measurement methods available [12]. Some of these include; the oversize boulder count method, sieving, visual

*Corresponding Author: yildirimozupak@email.com

Received 08 April 2022; Revised 16 May 2022; Accepted 20 May 2022

2687-5195 /© 2022 The Authors, Published by ACA Publishing; a trademark of ACADEMY Ltd. All rights reserved.

<https://doi.org/10.36937/ben.2022.4660>

analysis, shovel loading rate method, and image analysis method [11, 13-14]. WipFrag is an example of an image analysis method that will be adopted in this research for blast image analysis.

[16] indicated that spacing is the distance between adjacent drill hole rows. Blast design spacing is determined using the equation given below :

$$S = 1 \text{ to } 1.8 \times B \tag{1}$$

Where S denotes the drill hole spacing, B represents the drill hole burden distance, and a is the coefficient which [16] describes the value to usually varies from 1 to 1.8, 1 to 1.15 for general blasting, 1 for square drill pattern, 1.15 for staggered pattern, 0.7-1.0 for reinforcement stone (Rip-rap) [16]. Charge Length is calculate using the equation given below:

$$L = H - T + J \tag{2}$$

Where L denotes the drill hole charge length in m, H represents the drill hole length in m, T is the stemming length in m, and J is the sub drill in m.

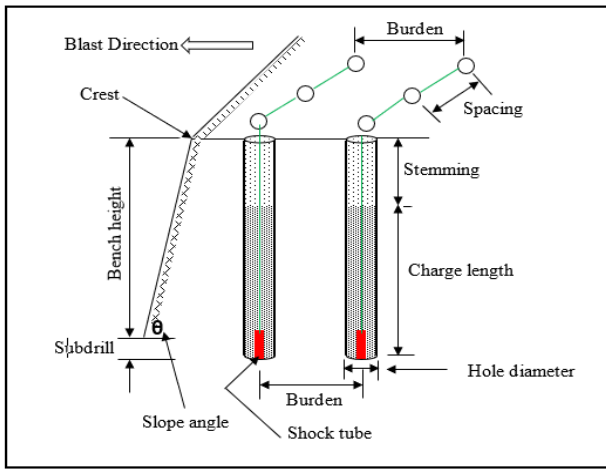


Figure 1. General layout of charge hole modified after [15]

[16] explains Sub drill as the length of the hole drilled extending below the mine bench floor level. [16] also established that sub drill guarantees a full-length blast hole will complete excavation down to the floor level. Sub drill is regularly 0.3 x burden or 8 to 12 hole diameters. Sub drill is calculated using the equations below:

$$J = 0.3 \times B \tag{3}$$

$$J = Kd \times De \tag{4}$$

Where B is the burden in m, De is the drill hole diameter, and Kd is the diameter ratio which ranges from 7 to 12 depending on the rock type.

Stemming length formed a confining seal over the explosive charge (Fig.1), holds in the detonation gasses until the explosive has detonated completely and the rock starts to break. The rule of thumb equations for calculating stemming length is given as below:

$$T = Kd \times De \tag{5}$$

$$T = Kb \times B \tag{6}$$

Where B is the burden in m, De is the drill hole diameter, Kd is the stemming to diameter ratio which ranges from 20 to 30 depending on the rock type and Kb is the stemming to burden ratio ranging from 0.2 to 1 [17].

$$T = Z \times \left(\frac{W \times REE}{100} \right)^{1/3} \tag{7}$$

Where Z denotes the Fly rock factor, which is select as 1 for normal blasting, and 1.5 for controlled blasting. W is the mass of explosives, REE is the Relative effective energy. Blasting operation efficiency requires several design adjustment between the controllable and uncontrollable factors. For instatnce, [17] and [18] noted that the drill hole height (H) must be more than stemming plus eight (T+8) times charge diameter to ensure there is no explosive blowout and fly rock during blast initiation. Stiffness ratio is define as the ratio of the drill hole height to burden distance. The striffness ratio of a blast is calculate using the quation below:

$$SR = \frac{H}{B} \tag{8}$$

Where H is the drill hole length in m, SR is the striffness ratio, and B is the burden in m

Table 1. Stiffness ratio effect on blast result [After 19]

Stiffness Ratio	1	2	3	4
Fragmentation	Poor	Fair	Good	Excellent
Airblast	Severe	Fair	Good	Excellent
Flyrock	Severe	Fair	Good	Excellent
Ground	Severe	Fair	Good	Excellent
Vibration				
Comments	Severe back break and toe problems	Redesign	Good control and fragmentation	No increased benefit by increasing stiffness ratio

The explosive powder Factor which is also described as the charge factor is defined according to [18] as the ratio of the total weights of explosives detonated during a blast divided by the quantity of rock broken. The charge factor is expressed as Kilogram per cubic meter (Kg/m³) [19]. [20] explained that as the powder factor in kg/m³ increases, the average fragment size decreases when the burden remains constant [20]. The powder factor for a single explosive charge column is calculated using the equation given below:

$$KS = \frac{W_e}{B \times S \times H} \tag{9}$$

Where W_e is the explosive charge weight per hole in kg, B denotes the blast hole burden in m, S represent the drill hole spacing in m, and H is the drill hole length in m. The powder factor for more than one explosive charge column per hole given as follows:

$$Lc = L - LB \tag{10}$$

$$Vc = \frac{\pi D^2}{4} \times Lc \tag{11}$$

$$VB = \left(\frac{\pi D^2}{4} \right) \times LB \tag{12}$$

$$WC = P1 \times Vc \tag{13}$$

$$WB = P2 \times VB \tag{14}$$

$$WT = WB + WC \tag{15}$$

$$KS = \frac{WT}{B \times S \times H} \tag{16}$$

Where, LB denotes the drill hole bottom charge length in m, Lc is the drill hole column charge length in m, VB denotes the volume of bottom charge in m³, π is denoted to be 22/7, P1 denotes the column charge explosive density in Kg/m³, P2 denotes the density of bottom charge explosive in Kg/m³, Vc is the volume of column charge in m³, D is the drill hole diameter in m, WB is the bottom charge weight in Kg, WC is the column charge weight in Kg, WT is the Total charge weight per hole in Kg, B is the burden, S denotes the spacing in m, H represents the drill hole length, and Ks denotes explosive charge

powder factor measured in Kg/m^3 . [21] work noted that WipFrag is an image analysis system for analysing the size of blasted or crushed rock piles among other materials. It has also been applicable to evaluating the particle distribution of ammonium nitrate prills, glass beads, and zinc concentrate for the proper concentration process. [22] indicated that WipFrag during processing measures image as 2-D net and reconstructs it into a 3-D distribution implementing the principle of Geometric probability. [23] established that WipFrag is a state-of-the-art image-based gravimetry system designed mainly for black and white (graytone) images, although it can accept also colored prints. Images are supplied to the software which transforms the image into a binary image consisting of a net of black outlines.

Achieving a well-distributed particle size is the main goal of blasting, so the rock is handled with efficiency in post-blast processes, e.g. loading and crushing. There are many factors that influences blasting result among which are; mechanical properties of rock mass, the pure geometry of blast holes, the number of explosives, initiation pattern, and delay times area unit among others are a number of the key factors in blast design as identified in [8] work. This study observes the influence of selected blast hole geometry and charges weight ratio on the efficiency of blasting results.

[24] noted that to obtain desired fragmentation size distribution from blast operation, sufficient design of the controllable blast factors is required to account for the uncontrollable factors such as rock strength and discontinuity properties t mention a few [25].

[24] observed stiffness ratio, powder factor and UCS of lafarge kanthan limestone to have a high correlation with the blast particle mean size. It was also noted that the ratio of the bench height to the burden ratio (stiffness ratio) increases with the 50% passing size. The study also revealed that the mean fragment size becomes finer as the powder factor increases [25] [26]. [25] work revealed that mean fragment size increases with stiffness ratio. In Sandeep et al work, it was also indicated that the optimal fragment size of rock depends on the blast design parameters and explosive parameters. Based on the various reviewed literature, the effect of blast design on small diameter drill hole blast fragmentation has not been investigated. This work investigates the effect of explosive bottom and column charge ratio and blast controllable factor design on small hole dolomite quarry blast.

2. Materials and methods

To accomplish the aim of this paper, a field study was completed at the Fanalou Dolomite Mining Lease 116 and Mining Lease 115. The case study quarry is situated in Ikpeshe, Akoko Edo local government Area, Nigeria on Longitude $07^{\circ}10'04''$ N, and latitude $06^{\circ}09'54''$ E and Longitude $07^{\circ}10'20''$ N and Latitude $06^{\circ}11'12''$ E. The mine bench works at 1.5 m and about 22.5 m depth drilled by a pneumatic Jackhammer in conjunction with 8.6Mpa (8.6 $\times 10^{-5}$ bar) pressure compressor. The mined rock mass rating was evaluated using [27] RMR rating, the formation has a rough surface, separation, no infilling, no fracture, unweathered wall rock surface, and persistence length of 1-3m. The rock comprises massive dolomitic marble with RMR 65 according to [28] rock mass classification. The mine blast hole diameter is 40mm. The mine uses the emulsion Dynogel product of Nigachem explosive manufacturer and ANFO as the blasting explosive. The company makes use of a staggered drilling pattern with Nigachem non-electric solacord having 6800 m/s VOD detonate instantaneously under No.6 detonator as the initiating cord. The density and UCS of the dolomite rock sample are 2600-2800 kg/m^3 and 44.42-54.6 MPa respectively (Table 2).

Table 2. Physio-mechanical properties of case study deposit

Location	UCS (Mpa)	Density Kg/m^3	Specific gravity	Colour	Rebound hardness value
Loc 1	44.42	2800.0	2.8039	Grey, white	38-46
Loc 2	54.65	2790.0	2.7900	White, brown	37-44
Loc 3	49.18	2672.7	2.6727	Grey, white	34-37

Fig. 2 and Fig.3 show the layout of Fanalou Dolomite Quarry and the general layout of the blast hole section respectively. For this study, basic blast parameters including burden, spacing, hole depth, drill hole diameter, stemming length, and bottom and column charge weight were measured for nine blast events. Using measured blast data, the ratio of the column and bottom charge weight (Wb/Wc) and specific charge (kg/m^3) were determined. Infield, after blasting, a 0.5m by 0.5m frame was used as a scaling object; the image of the blast muck piles for each blast was captured using a clear lens camera.



Figure 2. General overview of Fanalou Quarry

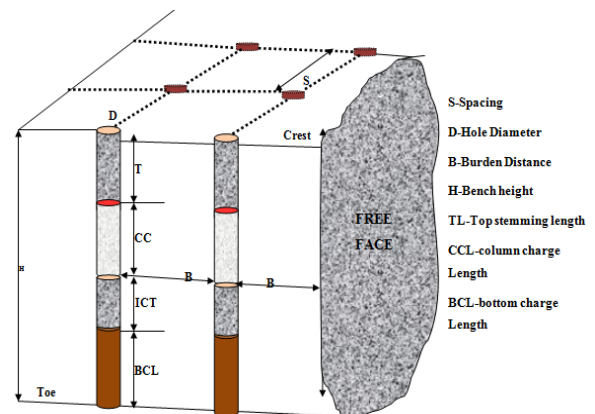


Figure 3. General layout of the blast hole section

The blast images captured from the site were imported into wipfrag© software for fragmentation analysis. The Image was delineated with an in-built editing and manual tools in the Wipfrag software. And the delineated images were sieved to get the fragmentation distribution curve and fragmentation sizes (mean fragment size X_{50} , m, and X_{80} , m) were determined. Fig. 5 and 6 show two of the blast image netting with the distribution curves generated from the Wipfrag software.

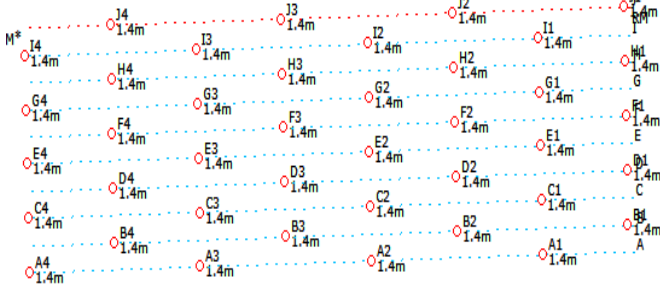


Figure 4. Diagonal firing pattern of blast 8

3. Results and discussion

Nine blasting operations in two different Dolomite Quarry pits were used for this study with different blast design parameters. Fig. 5-6 shows the Wipfrag analysis result for Blast 7 and 8 respectively.

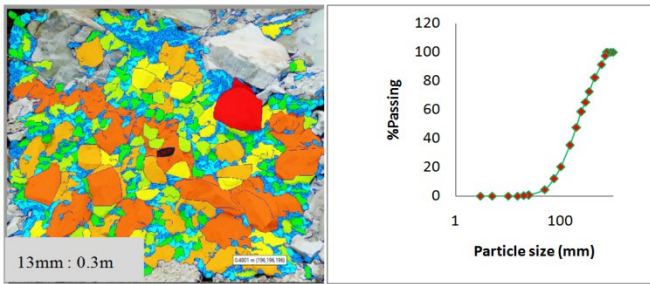


Figure 5. Blast 7 Fragmentation analysis and the distribution curve

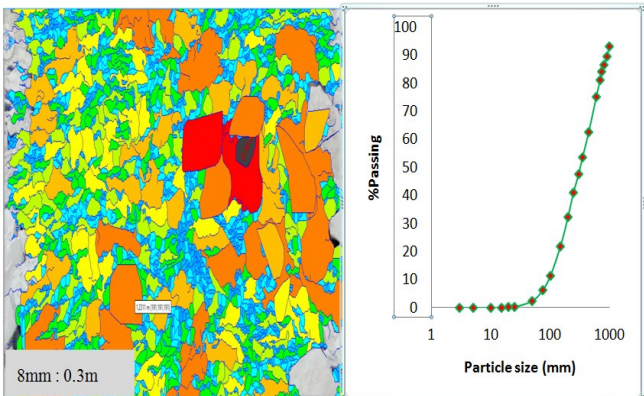
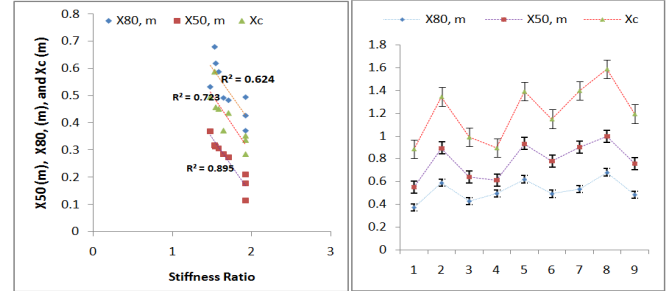


Figure 6. Blast 8 Fragmentation analysis and the distribution curve

3.1 Relationship between blast stiffness ratio (H/B) and the fragment sizes distribution

Fig. 7 shows that, blast fragment particle size (mean size, X_{50} , greatest part size (X_{80}), and characteristic size (X_c) declines as the blast design stiffness ratio increases in a similar direction to [28] findings. Besides, it likewise uncovers that there is an extraordinary decrease in the fragment particle size. The work of [29] likewise revealed that an increase in stiffness ratio makes the bench fragmentation rate more flexible, producing better fragmentation. Also [30] noted that small stiffness ratio results in greater stiffness in energy distribution, which in turn, offers greater resistance to fracturing rate in bench blast results. [31] noted poor breakage along the drill hole collar region during charge initiation to be attributed to the increased bench stiffness.



(a) (b)

Figure 7. Relationship between stiffness ratio (H/B) and rock fragment sizes (mean size X_{50} , (m), Maximum size X_{80} , (m), and Characteristic size X_c (m))

$$X_{80} = -0.410SR + 1.217 \tag{17}$$

$$X_c = -0.425SR + 1.142 \tag{18}$$

$$X_{50} = -0.410SR + 0.960 \tag{19}$$

Where, X_{80} denotes the blast result 80% passing size, X_{50} represents the blast fragmentation 50% passing size, X_c is the characteristic size, and SR denotes the blast design stiffness ratio. The R^2 value obtained from Fig. 7a shows the correlation between the actual value and the predicted value of fragmentation size distribution from the developed linear models. [32] indicated that the degree of model accuracy is define by the closeness of the of R^2 value to unity. The R^2 value obtained using Equations developed above for the prediction of X_{80} , X_{50} , and X_c are 0.624, 0.723, and 0.895 respectively and it is suitable for predicting blast fragment size distribution in quarry pre-blast design.

3.2 Relationship between rock fragment sizes distribution and bottom charge to column charge ratio (W_b/W_c)

From Fig. 8, the blast fragment particle size (mean size, X_{50} , maximum fragment size (X_{80}), and characteristic size (X_c) of the blasted rock increases as the ratio of explosive bottom charge to column charge increases. This may be due to an increase in the high-pressure shockwave, which is then followed by a rapid increase in gas pressure generated from the high explosive bottom charge which supports high tensile slabbing [33].

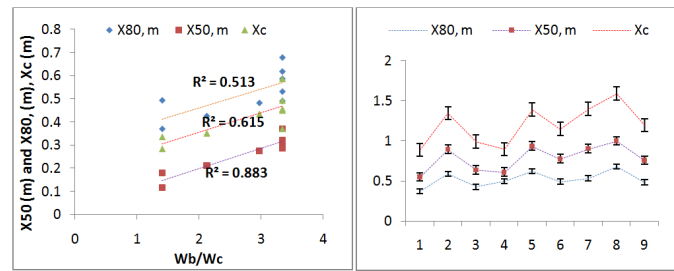


Figure 8. Relationship between bottom charge to column charge ratio (W_b/W_c) and rock fragment sizes (Mean size X_{50} (m), maximum

$$X_{80} = 0.080Wr + 0.300 \tag{20}$$

$$X_c = 0.085Wr + 0.186 \tag{21}$$

$$X_{50} = 0.088Wr + 0.021 \tag{22}$$

Where, X_{80} denotes the blast result 80% passing size, X_{50} represents the blast fragmentation 50% passing size, X_c is the characteristic size, and Wr is the Charge weight ratio.

The R^2 value obtained using the above developed equations for the prediction of the mine blast X_{80} , X_{50} , and X_c particle size distribution are 0.513, 0.615, and 0.883 respectively, and are suitable for predicting blast fragment size distribution in the quarry.

3.3 Relationship between rock fragment size and the explosive specific charge

Fig. 9 shows that, the blast fragment particle size (mean size, X_{50} , maximum fragment size (X_{80}), and characteristic size (X_c) of the blasted rock decreases with increase in the explosive specific charge. This is in alignment with [6] findings in Bharat coking coal field limited situated at Dhanbad, Jharkhand India and [34] findings in Lanfarge Kanthan Limestone quarry. This study reveals that mine explosive specific charge increases from 0.70-0.97 kg/m³, the mean fragment size X_{50} varies from 0.12-0.37, maximum fragment size (X_{80}) varies between 0.37-0.68, and characteristic size (X_c) varies between 0.28-0.59.

$$X_{80} = -0.410K + 1.217 \tag{23}$$

$$X_c = -0.425K + 1.142 \tag{24}$$

$$X_{50} = -0.410K + 0.960 \tag{25}$$

Where, X_{80} denotes the blast result 80% passing size, X_{50} represents the blast fragmentation 50% passing size, X_c is the characteristic size and K denotes the specific charge in kg/m³. The R^2 value obtained using Equations developed above for the prediction of the blast X_{80} , X_{50} , and X_c particle size distribution are 0.624, 0.723, and 0.895 respectively and it is suitable for predicting blast fragment particle size distribution quarry.

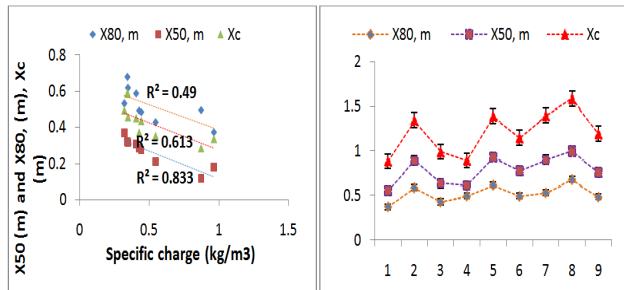


Figure 9. Relationship between specific charge and rock fragment sizes (mean size X_{50} (m), maximum size X_{80} (m), and Characteristic size X_c (m))

3.4 Empirical Models for the prediction of Blast fragmentation

Multivariate Regression modeling method was adopted for developing the proposed models in this study. Three different Multivariate regression (MVR) models were developed predicting each of X_{80} , X_{50} , and X_c . Three input variables representing the stiffness ratio (SR), Specific charge (K), and the Maximum instantaneous charge (MIC) were used in each of the models as shown in Table 3. The model input and output variables elements were normalized (scaled) between -1 and 1 using Equation below to achieve dimensional consistency in the variable elements and also to eliminate over-fitting during model training.

$$X_i = \frac{2(P_i - P_{min})}{(P_{max} - P_{min})} - 1 \tag{26}$$

Where X_i is the normalized elements, P_i is the actual data to be normalized; P_{max} and P_{min} are the maximum and minimum values of the actual data set, respectively.

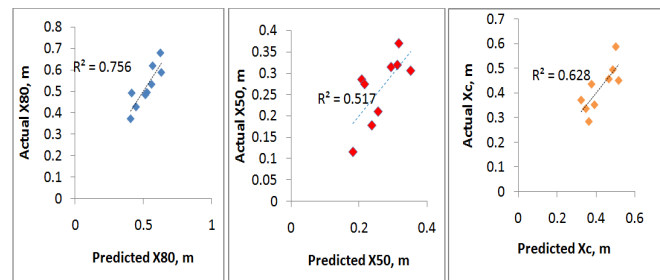


Figure 10. Relationship between the Model Predicted and Wipfrag Measured blast fragmentation size distribution

Table 3. Blast design Parameters and blast fragmentation data set for MVR Model development

Blast ID	SR	PF	MIC	X_{80} , m	X_{50} , m	X_c , m
Blast 1	1.357	0.9696	43.52	0.37146	0.1776	0.3368
Blast 2	1.357	0.9736	39.33	0.58797	0.3056	0.45108
Blast 3	1.159	0.9075	43.98	0.42691	0.2099	0.35249
Blast 4	1.227	0.7045	39.17	0.4948	0.1155	0.28478
Blast 5	1.158	0.8631	43.71	0.61917	0.3142	0.45714
Blast 6	1.428	0.9249	48.08	0.492	0.2850	0.37146
Blast 7	1.071	0.8894	43.71	0.53258	0.3696	0.4948
Blast 8	1.146	0.8400	39.33	0.67959	0.3191	0.58797
Blast 9	1.315	0.8090	31.97	0.48341	0.2741	0.43594

The final mathematical MVR models were de-normalized using the Equation given below:

$$P_i = \frac{P_{max} - Y_{max}}{2} X_p + \frac{P_{max} + P_{max}}{2} \tag{27}$$

Where X_p denotes the MVR predicted elements, P_i is the actual predicted data de-normalized; P_{max} and P_{min} are the maximum and minimum values of the measured data, respectively.

The de-normalized final MVR models are shown below:

$$X_{80} = 0.1541[0.081SR - 0.052K - 0.723MIC - 0.042] + 0.526 \tag{28}$$

$$X_{50} = 0.127[-0.165SR + 0.506K - 0.441MIC + 0.006] + 0.234 \tag{29}$$

$$X_c = 0.152[-0.163SR + 0.294K - 0.551MIC - 0.218] + 0.436 \tag{30}$$

The respective coefficient of determination of the developed MVR models for each blast fragmentation particle size is illustrated in Fig. 10. The R^2 values from the developed model test for the blast X_{80} , X_{50} , and X_c particle size distribution are 0.76, 0.52, and 0.63 respectively. The proposed MVR models are suitable for the prediction of blast fragmentation particle size distribution.

4. Conclusions

The influence of blast design factors and Explosive charge load on the blast fragment size distribution has been studied. The stiffness ratio, the bottom charge to column charge ratio, and the specific charge are considered factors with great influence on blast particle size distribution. An average spacing of 1m, burden of 0.8m, stemming length of 0.65, column charge weight of 0.252 kg, bottom charge weight of 0.633 kg, the specific charge of 0.873kg/m³, and stiffness ratio of 1.69 as utilized in Golden girl quarry produces 1.45 to 1.55 uniformity index for all nine blast events. The X_{50} size obtained in all nine blast events analyzed ranges from 180 mm to 320 mm for a primary crusher of 350 mm gape opening. The Wipfrag analysis result for all the blasts reveals that about 56% of the blast event assessed produced good fragmentation. The following conclusions are drawn from the study:

- ❖ The blast fragment size (50% and 80% mesh undersize size materials) and characteristic size decrease with stiffness ratio and decrease with increases quantity of specific charge (m³/kg).
- ❖ Mean fragment size X_{80} , X_{50} , and characteristic size X_c increase with an increase in the ratio of bottom charge to column charge.
- ❖ Multivariate Regression (MVR) models were developed for the prediction of blast fragmentation sizes (X_{80} , X_{50} , and X_c) with R^2 values of 0.76, 0.52, and 0.63 respectively. Based on the low

correlation value obtained from the developed models, the proposed multivariate Regression (MVR) models are less suitable for the prediction of blast fragmentation particle size distribution. Further research should also include rock mass properties, initiation sequence and timing, the orientation of discontinuities, and the influence of explosives characteristics on blast fragmentation.

Acknowledgement

The author wishes to register his gratitude to Engr. Abdulkadir (School Mines, China University of Mining & Technology, Xuzhou China) for reading the first draft of the article. The author also acknowledges Fanalou Company for their technical support in data acquisition for this research work.

Declaration of Conflict of Interest

The author declares that there is no conflict of interest. He has no known competing financial interests or personal relationships that could have appeared to influence the work reported in this paper.

References

- [1.] Brady, B. H. G., Brown, E. T., Energy changes accompanying underground mining. In: *Rock Mechanics*. Springer: Dordrecht, (1998), pp. 240-259.
- [2.] Mackenzie, A. S., Cost of explosive – do you evaluate it properly. *Mining Congress Journal*, 52(5), (1996), pp. 32-41.
- [3.] Melodi, Mbuyi M., Blessing O. Taiwo, and Itunu O. Ajayi. "Evaluation of Granite Production and Market Structure for the Improvement of Sales Performance in Ondo and Ogun States, Southwest Nigeria." *FUOYE Journal of Engineering and Technology (FUOYEJET)* 7, No. 1 (2022): 75-79.
- [4.] Hustrulid, W., *Blasting Principles for Open Pit Mining*, Volume 1-General Design Concepts: A.A.Balkema,(1999), 812p.
- [5.] Kanchibotla, S. S., Optimum blasting? Is it minimum cost per broken rock or maximum value per broken rock?. *Fragblast*, 7(1), (2003), pp.35-48.
- [6.] Prasad, S., Choudhary, B. S., Mishra, A. K., Effect of stemming to burden ratio and powder factor on blast induced rock fragmentation—a case study. In: *IOP conference series: materials science and engineering*. IOP publishing, 225(1), (2017), pp. 12-191.
- [7.] Dinis, C., Da Gama, C., Lopez J., Rock Fragmentation control for Blasting cost minimization and environmental impact a battement, In: *Proceedings of the 4th International Symposium On Rock Fragmentation by Blasting (Fragblast-4)*, Vienna:Austria, (1993), pp. 273-280.
- [8.] Tiile, R. N., *Artificial neural network approach to predict blast-induced ground vibration, Airblast and rock Fragmentation*. Masters Theses. Missouri university of science and Technology, Faculty of the Graduate School, Department of Mining Engineering: Missouri, (2016), 91 p.
- [9.] Dick, R. A., Fletcher, L. R., D'Andrea, D. V. (1983): *Explosives and blasting procedures manual* (No. 8925). US Department of the Interior, Bureau of Mines.
- [10.] Muhammed, A. R., *The Effect of Fragmentation Specification on Blasting Cost*. Unpublished MSc Thesis Report, Queen's University, Kingston, Ontario, Canada, (2009), 200 p.
- [11.] Adel, G., Kojovic, T., Thornton, D. (2006): *Mine-to-mill optimization of aggregate production*. Virginia Polytechnic Institution and State University Virginia Tech, Blacksburg, VA United States, (2006).
- [12.] Paley, N. A., Adjusting Blasting to Increase SAG Mill Throughput at the Red Dog mine. In: *Proceedings of the 27th ISEE Annual Conference*, Orlando. (2001), pp. 65-80.
- [13.] Grundstrom, C., Kanchibotla, S., Jankovich, A., Thornton, D., Pacific, D. D. N. A., Blast Fragmentation for maximizing the sag mill throughput at Porgera Gold Mine. In: *proceedings of the annual conference on explosives and blasting technique*, Porgera,(2001), pp. 383-400.
- [14.] Valery W., Morrell, S., Kojovic, T., Kanchibotla, S.S., Thornton, D.M., Modeling and Simulation Techniques Applied for Optimisation of Mine to Mill Operations and Case Studies. *CETEM/MCT, Rio de Janeiro, Brazil*, (2001), pp.107-116.
- [15.] Shaib, A. S., Mohd, H. M., Nur Aliah, H. A., Preliminary Assessment of The Effects of Blast Design Factors on Fragmentation at Lafarge Kanthan Limestone Quarry, Chemor, Perak. *ASEAN Engineering Journal*, 10(2), (2020), pp.58-79.
- [16.] Mishra, A., *Design of Surface Blast – A Computational Approach*. Unpublished Bachelor of Technology Project Report, National Institute of Technology, Rourkeda, India, (2009), pp.11
- [17.] Sharma, P.D., Controlled Blasting Techniques – Means to mitigate adverse impact of blasting in Open pits, Quarry, Tunnel, UG metal mines and construction workings; *Mining Engineers' Journal* (2008), pp.14-22.
- [18.] Konya, C.J. Blast Design, *Intercontinental Development Corporation, Ohio 44064*, USA. (1995).
- [19.] Bhandari, S., *Engineering Rock Blasting Operations*. A.A. Balkema, Rotterdam, Brookfield, (1997), 375p.
- [20.] Gustafsson, R., *Blasting Technique*. Dynamite Noble, (1981), pp.81-89, 121-127.
- [21.] Palangio, T. C., WipFrag - A new Tool For Blast Evaluation. In: *Proceedings. 11th Annual ISEE Symposium On Blasting Research*, Nashville, Tennessee, (1985), pp. 269-285.
- [22.] Maerz, N. H., Reconstructing 3-D Block Size Distributions from 2-D Measurements on Sections. In: *Proceedings of the ISRM/Fragblast 5 Workshop and Short Course on Fragmentation Measurement* . Montreal, A. A. Balkema. (1996a).
- [23.] Maerz, N. H., Image Sampling Techniques and Requirements for Automated Image Analysis of Rock Fragments. In: *Proceedings of the ISRM/Fragblast 5 Workshop and Short Course on Fragmentation Measurement* . Montreal, A. A. Balkema. (1996a).
- [24.] Abdulazeez Shehu, S., Hazizan, M., Hashim, M., Aliah, N., and Kechik, H. A. (2020). Preliminary Assessment of the Effects of Blast Design Factors on Fragmentation at lafarge kanthan limestone quarry, chemor, perak. In *ASEAN Engineering Journal* Vol. 10 (2), P.58.
- [25.] Prasad, S., Choudhary, B. S., and Mishra, A. K. (2017). Effect of Stemming to Burden Ratio and Powder Factor on Blast Induced Rock Fragmentation– A Case Study. *IOP Conference Series: Materials Science and Engineering*, Vol. 225, pp.1-9. <https://doi.org/10.1088/1757-899x/225/1/012191>
- [26.] Mohamed, F., Hafsaoui, A., Talhi, K. and Menacer, K. (2015). Study of the powder factor in surface bench blasting, *Procedia Earth and Planetary Science*, Vol. 15, pp. 892-899 doi:10.1016/j.proeps.2015.08.142
- [27.] Bieniawski, Z. T., *Engineering Rock Mass Classifications*. In A Complete Manual for Engineers and Geologists in Mining, Civil and Petroleum Engineering test Standard, John Wiley and Sons publisher, Toronto. (1989).
- [28.] Rai, P., Ranjan, A. K., Singh, B., Optimizing Fragmentation-A study of the impact of stiffness ratio on the fragmentation of sandstone strata in an opencast coal mine. *Quarry Management*, 3(2), (2005), pp.33-38.
- [29.] Smith, N.S., *Burden rock stiffness and its effects on fragmentation in bench blasting*. Ph.D. Thesis. University of Missouri, USA, (1976), 163p.
- [30.] Lundborg, N., Persson, A., Ladegaard-Pedersen, A., Holmberg, R., Keeping the lid on flyrock in open-pit blasting. *Engineering Mining Journal*, 17(6), (1975), pp.95-100.
- [31.] Rai, P. *Evaluation of the effects of some blast design parameters on fragmentation in opencast mines*. Ph.D. Thesis, Banaras Hindu University, Varanasi. (2002), 27p.
- [32.] Spiess, A. N., and Neumeyer, N. An evaluation of R² as an inadequate measure for nonlinear models in pharmacological and biochemical research: a Monte Carlo approach. *BMC pharmacology*, 1(1), (2010), pp. 1-11.
- [33.] Konya, A. J., *The mechanics of precision presplitting The mechanics of precision presplitting*. Ph.D. Thesis. . University of Missouri, USA, (2019), 207p.
- [34.] Abdulazeez, S. S., Hazizan, M., Hashim, M., Aliah, N., Kechik, H. A., Preliminary assessment of the effects of blast design factors on fragmentation at lafarge kanthan limestone quarry, chemor, perak. *ASEAN Engineering Journal*, 10(2), (2020) pp. 13-23.

How to Cite This Article

Taiwo, B.O., Effect of charge load proportion and blast plan on blast fragment size appropriation, *Brilliant Engineering*, 3(2022), 4660. <https://doi.org/10.36937/ben.2022.4660>